Automated Lightning Flash Detection in Nighttime Visible Satellite Data

RICHARD L. BANKERT, JEREMY E. SOLBRIG, AND THOMAS F. LEE

Naval Research Laboratory, Monterey, California

STEVEN D. MILLER

CIRA, Colorado State University, Fort Collins, Colorado

(Manuscript received 27 July 2010, in final form 6 December 2010)

ABSTRACT

The Defense Meteorological Satellite Program (DMSP) Operational Linescan System (OLS) nighttime visible channel was designed to detect earth–atmosphere features under conditions of low illumination (e.g., near the solar terminator or via moonlight reflection). However, this sensor also detects visible light emissions from various terrestrial sources (both natural and anthropogenic), including lightning-illuminated thunderstorm tops. This research presents an automated technique for objectively identifying and enhancing the bright steaks associated with lightning flashes, even in the presence of lunar illumination, derived from OLS imagery. A line-directional filter is applied to the data in order to identify lightning strike features and an associated false color imagery product enhances this information while minimizing false alarms. Comparisons of this satellite product to U.S. National Lightning Detection Network (NLDN) data in one case as well as to a lightning mapping array (LMA) in another case demonstrate general consistency to within the expected limits of detection. This algorithm is potentially useful in either finding or confirming electrically active storms anywhere on the globe, particularly those occurring in remote areas where surface-based observations are not available. Additionally, the OLS nighttime visible sensor provides heritage data for examining the potential usefulness of the Visible-Infrared Imager-Radiometer Suite (VIIRS) Day/Night Band (DNB) on future satellites including the National Polar-orbiting Operational Environmental Satellite System (NPOESS) Preparatory Project (NPP). The VIIRS DNB will offer several improvements to the legacy OLS nighttime visible channel, including full calibration and collocation with 21 narrowband spectral channels.

1. Introduction

Polar-orbiting satellite data have been available from the Defense Meteorological Satellite Program (DMSP) for over 40 years. The Operational Linescan System (OLS), on board the DMSP satellites, is a two-channel radiometer with visible and infrared (IR) data sensors. A high-gain amplifier (photomultiplier tube) offers high sensitivity and a unique ability to image low levels of visible light (Miller and Turner 2009; Isaacs and Barnes 1987). The OLS nighttime visible channel was originally designed for cloud and snow cover imaging in reflected moonlight, including full moon and lunar phases as low as first- and third-quarter moons. It was soon realized that OLS imagery also contained potentially valuable information about visible light emission features. As noted in Fig. 1 (from Lee et al. 2006), light emission sources, including city lights, fires, highway lighting, fishing boats, and streaks related to cloud tops illuminated by lightning flashes, appear as bright features, particularly when viewed in the absence of moonlight. Most of these features can also be seen, albeit more faintly, in the presence of abundant moonlight. By utilizing this sensitivity of the OLS to visible emission sources, we develop an automated lightning detection algorithm that can be applied in varying degrees of lunar illumination in addition to being applied in the absence of moonlight.

Lightning information in OLS imagery has been underutilized due to the difficulty in isolating the signal. This detection algorithm enhances lightning flash signatures while suppressing background information. Operationally, the lightning product is useful for finding or confirming electrically active storms anywhere on the globe and particularly those occurring in remote areas

Corresponding author address: Richard Bankert, Naval Research Laboratory, 7 Grace Hopper Ave., Monterey, CA 93943-5502.
E-mail: rich.bankert@nrlmry.navy.mil

DOI: 10.1175/WAF-D-10-05002.1

FIG. 1. The OLS nighttime visible features detected (a) with and (b) without moonlight (from Lee et al. 2006).

where surface-based observations are not available or are unable to account for intracloud lightning. Analysis and forecasting of tropical cyclone intensity can be aided by improved knowledge of lightning flash locations within these systems (Demetriades et al. 2010; DeMaria and DeMaria 2009) while lightning identification, in general, can provide an indication of phase-stratified cloud features and, therefore, cloud with aircraft icing potential (Bernstein et al. 2005).

As a DMSP satellite passes over a thunderstorm, the OLS is able to record lightning flashes with its nighttime visible band. To an astronaut viewing a thunderstorm from a space shuttle or the International Space Station, lightning flashes appear at cloud top as a brief and diffuse illumination of the parent cloud system. A scanning radiometer such as the OLS observes this behavior in a different way, with the transient flash event captured as a ''streak'' along the direction of the sensor's scan (Orville and Henderson 1986; Orville 1981). The streak patterns are due to the cross-track scanning pattern of the OLS and the sustained flickering of multiple return strokes associated with one or more cloud-to-cloud or cloud-to-ground flashes. Figure 2 (from Miller et al. 2008) is an example of a nighttime visible and infrared bispectral composite showing various sources of emitted light, including lightning flashes. This enhancement depicts sources of nighttime visible light as either yellow (when the corresponding infrared brightness temperature is warm) or white (when the temperature is cold). Cold cloud tops are shown in blue. The lightning flashes in Fig. 2 appear as along-scan-line white streaks in the nighttime visible imagery, while cities and fires show up as bright areas of varying size, and highways appear as broken, curvilinear features that typically are not oriented along the direction of the OLS scan lines.

Although limited in its application, the OLS may complement the information provided by surface-based observations. The scanning OLS detector views a small area at any given time and is not designed to constantly monitor a large region like a lightning detection network. As a result only a small fraction of the total lightning occurring in

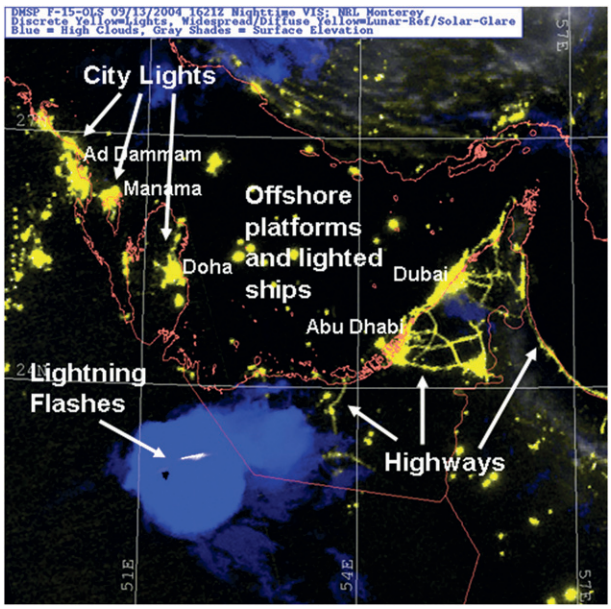

FIG. 2. The OLS nighttime bispectral color composite over the Arabian Peninsula and Persian Gulf at 1621 UTC 13 Sep 2004. The nighttime visible channel is cast in the red (R) and green (G) guns, and the longwave IR is cast in the blue (B) gun.

a given storm is captured in the image. Orville and Henderson (1986) estimated that about one in every 10^5 lightning flashes is recorded by OLS. However, the OLS detects intracloud lightning flashes, which are known to be more frequent than the cloud-to-ground flashes observed by surface-based systems such as the National Lightning Detection Network (NLDN). Depending on region, the ratio of intracloud to cloud-to-ground flashes over land is estimated to range from 0.5 to nearly 10.0 with an average of approximately 3.0 (Boccippio et al. 2001). Lightning mapping arrays (LMA) and Lightning Detection and Ranging (LDAR) networks can detect total lightning, but only for limited areas of coverage.

An objective technique for the detection and display of OLS-detected lightning flashes under various conditions of lunar illumination is developed in this research. This illumination can be a source of contamination and potential false alarms to the algorithm. The technique complements existing terrestrial-based lightning detection networks by providing the serendipitous detection of cloud electrification in remote locations. Within this paper, additional details concerning the DMSP OLS observing system can be found in section 2. The automated lightning detection algorithm is described in section 3 and an example of how the product can be visualized in enhanced imagery is presented in section 4. Finally, a summary of the current work and discussion of future applications for next-generation low-light imagers can be found in section 5.

2. DMSP OLS

Satellites in the DMSP constellation fly in sun-synchronous orbits at 830-km altitude with 101-min periods. The DMSP OLS, designed for day–night cloud analysis, is equipped with a two-channel [0.6 μm visible and 11.0 μm infrared (IR)] imager and a photomultiplier tube attached to the visible channel for low-light imaging over a 3000-km swath. The swath is constructed by a cross-track (perpendicular to the ground track of the satellite) scanning pattern where individual elements of each scan line are represented as discrete pixels of information on either visible brightness or radiometric temperature. The nighttime visible channel actually covers a portion of both the visible and near-IR regions of the electromagnetic spectrum (Lee et al. 2006; Elvidge et al. 1998b). As discussed earlier, the ability to detect low-light features makes the OLS unique and its data provide a useful resource for additional applications.

An element of the OLS that distinguishes it from other satellite imagers is its scanning strategy. While some imagers [e.g., the Advanced Very High Resolution Radiometer (AVHRR) and the Moderate Resolution Imaging Spectroradiometer (MODIS)] have degraded spatial resolutions away from nadir, the OLS mechanically reduces the physical size of its detector at prescribed scan angles to minimize this degradation and allow for improved image sharpness near the scan edge (Elvidge et al. 1998a, 1997). To preserve signal strength as the detector size decreases toward the edge of a scan, the OLS implements a ''pendulum motion'' scan that effectively increases the dwell time at the scan edges.

There are two spatial resolutions available to the OLS: smooth (2.7-km pixels) and fine (0.56-km pixels). Fine-resolution data are never available for both the visible and IR channels at the same time. Typically, the IR channel produces fine-resolution data at night and smooth resolution data during the day, while the opposite is true for the visible channel. As a consequence, fine visible data are rarely available over nighttime scenes. Even when fine-resolution nighttime visible imagery is available, there are inherent limitations to the sensor's actual ability to produce high spatial resolution images (Lee et al. 2006). Despite the higher sampling rate of the fine mode, large, overlapping instantaneous fields of view (IFOVs) greatly limit the sharpness and detail of the imagery. The examples shown in this paper are from the smooth-resolution nighttime visible data.

3. Automated lightning detection

Although coarse radiometric resolution (6-bit data or 64 gray shades) and the lack of a standard calibration limit the application of the OLS nighttime visible channel mainly to qualitative imagery (Miller and Turner 2009), this research makes use of the gradient edges within the data to produce an automated lightning detection algorithm. As such, the algorithm does not require absolute calibration, but depends upon the relative contrast against the surrounding scene—a requirement that presents various difficulties in the presence of certain anthropogenic light features (e.g., roads and cities) and side illumination of clouds by moonlight, which may on occasion appear as ''bright linear features'' oriented along the scan lines of the OLS imagery.

As noted earlier and seen in Fig. 3, lightning flashes appear in OLS nighttime visible imagery as bright streaks oriented along the scan line. These streaks usually do not depict the exact locations of lightning discharges, but are artifacts of a cloud top that is undergoing transient illumination by the upward diffusion of a lightning flash occurring somewhere within the cloud (Lee et al. 2006). In this imagery, lightning is noted as a bright discontinuity along a scan line, which typically does not extend into adjacent scan lines due to the brevity of most lightning flashes and the relatively long scan rate ($\sim$0.42 s per scan line) for

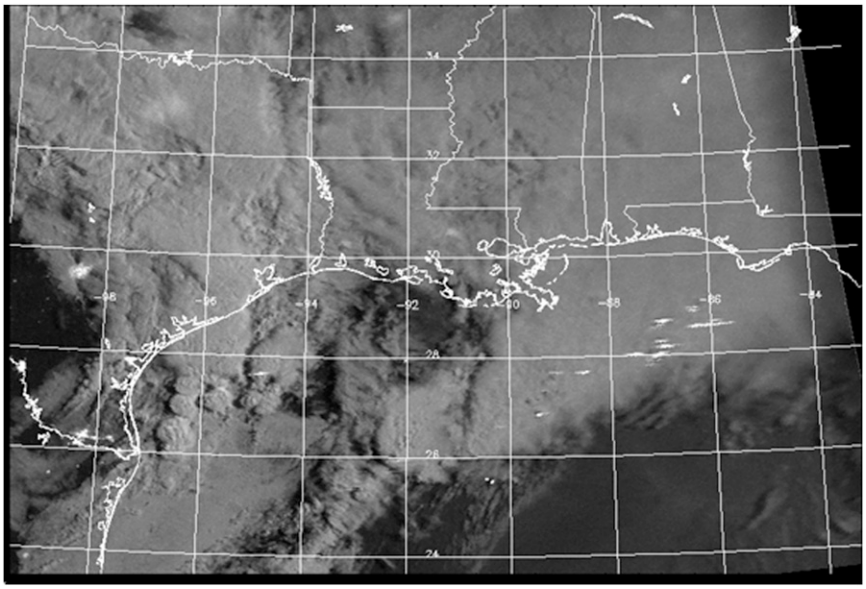

FIG. 3. The OLS nighttime visible image over Gulf of Mexico region at 0126 UTC 2 Dec 2009. Lightning flashes appear as white streaks along the scan lines. Some flashes are relatively dim and difficult to identify.

OLS. Thus, this signature typically appears as a bright linear feature in the direction of scanning regardless of the location or orientation of the lightning itself. The bright, linear discontinuity makes automated identification a good candidate for established line-filtering methods.

Earlier research efforts (Scharfen 1999) aimed at developing an automated lightning detection system used historical OLS data and other contextual information to develop, train, and test four separate neural networks that identify lightning signatures in the imagery. Each network was developed for a distinct moon phase. For the current research, we apply a line detection method that is applicable under all lunar illumination conditions. The detection method represents the second derivative of the image data. More specifically, the application of a directional filter (convolution kernel)—oriented in the direction of the lightning streaks—is used to single out the along-scan-line gradients of the OLS data. The convolution kernel applied here takes the form of an 11 × 3 filter:

-1	-1	-1	-1	-1	-1	-1	-1	-1	-1	-1
2	2	2	2	2	2	2	2	2	2	2
-1	-1	-1	-1	-1	-1	-1	-1	-1	-1	-1

The size and magnitude of this line-directional filter evolved through experimentation to reveal relatively faint and short lightning streaks that might otherwise go undetected, by a human analyst, as well as the more obvious (long, bright) streaks. Convolving this filter to the nighttime visible data results in an image on which lightning and other line-directional edges stand out. Example OLS nighttime visible and IR images are displayed in Figs. 3 and 4, respectively. The result of the line detection filter applied to the nighttime visible image data in Fig. 3 is displayed in Fig. 5. Only positive values are displayed as they correspond to pixels that are significantly brighter than neighboring scan-line pixels in the nighttime visible imagery. The most obvious lightning flashes seen in the visible image are also easily seen in the filtered image. In addition, several flashes that were less obvious are now highlighted in the filtered image.

4. Product demonstration and analysis

The OLS lightning flash detection product is useful for qualitative applications, such as enhanced imagery, which is designed to assist human analysts in understanding the presence of lightning within the context of other aspects of a meteorological situation (e.g., identifying the most intense embedded convective regions of a large mesoscale convective complex). In this section, we present examples of the current lightning detection product within the context of value-added imagery and compare against surface observations.

a. False color imagery product

There are three principal considerations for designing an enhanced lightning detection image. First, the relatively small lightning features must be made to stand out against

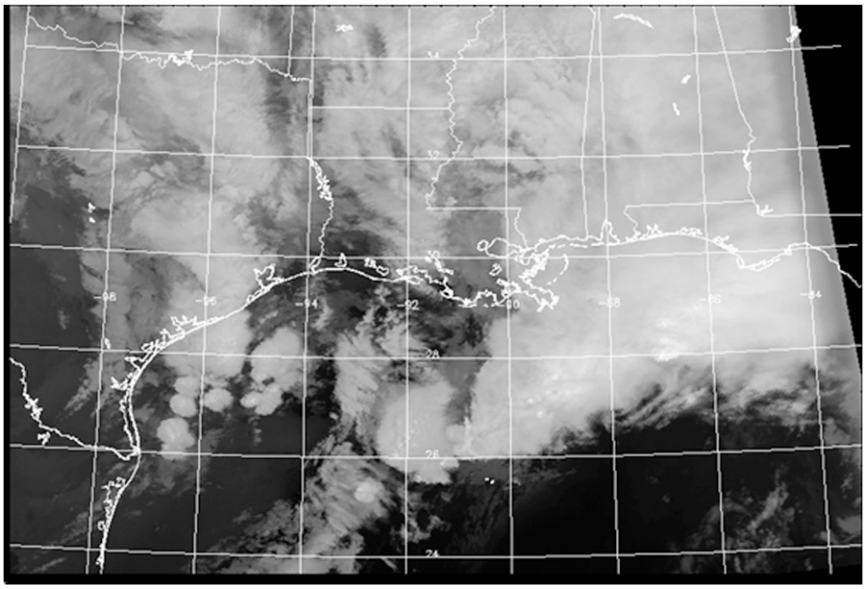

FIG. 4. The OLS IR image over Gulf of Mexico region at 0126 UTC 2 Dec 2009. Low brightness temperatures are bright (high cloud tops). High brightness temperatures are dark.

other features in the imagery (e.g., cities, clouds, etc). Second, the image should aid the analyst in identifying lightning by eliminating–reducing the visual impacts of false detections that may still exist after filter application. Third, the method should be capable of identifying lightning independent of background temperature, surface visible background brightness, and geographic location.

To achieve all three goals simultaneously, a false color imagery product was developed (Fig. 6) based on a combination of the raw nighttime visible data (Fig. 3), the IR data (Fig. 4), and the lightning (LGT) image data (Fig. 5). The input nighttime visible (VIS), IR, and LGT image data are scaled to range between 0 and 255 to create three separate 8-bit images.

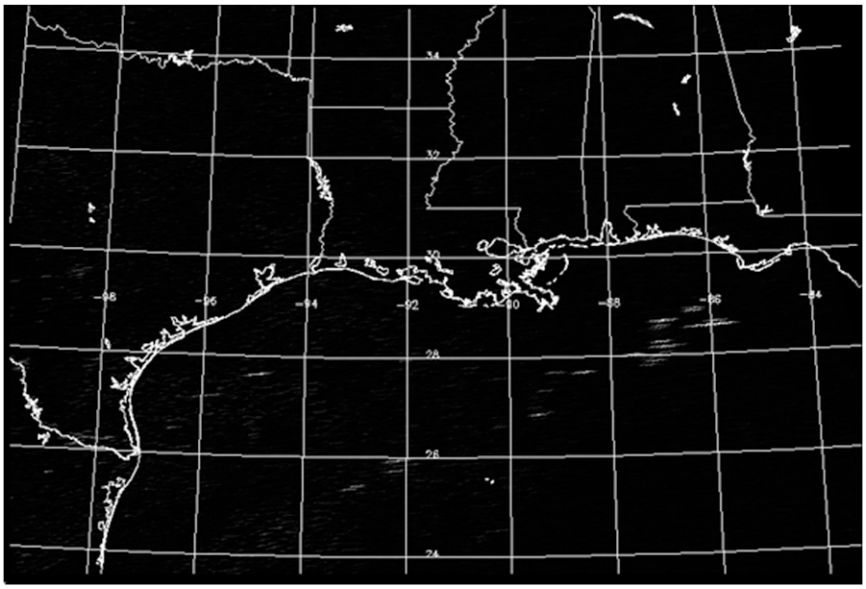

FIG. 5. Detected lightning image at 0126 UTC 2 Dec 2009. The image was created by applying an 11 × 3 convolution kernel to the nighttime visible data. Some lightning flashes are more apparent than in the nighttime visible image.

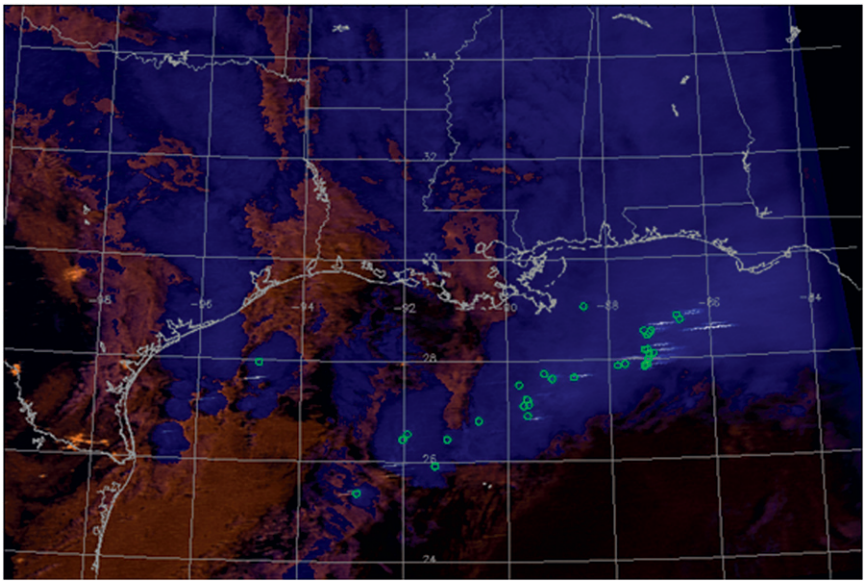

FIG. 6. The RGB composite image of nighttime VIS, IR, and detected LGT imagery data at 0126 UTC 2 Dec 2009 with NLDN lightning detection points indicated by green circles. Only those NLDN records that occurred within 5 s and 20 km of the time and location, respectively, of any OLS pixels within the region are marked.

For the false color imagery, the red (R), green (G), and blue (B) color values (collectively RGB), which are combinations of the three images, are determined in the following manner:

$$R = \begin{Bmatrix} \mathrm{LGT} & \text{if} \quad \mathrm{IR} < -25^\circ\mathrm{C} \\ \dfrac{255(\mathrm{VIS} + \mathrm{LGT})}{\max(\mathrm{VIS} + \mathrm{LGT})} & \text{if} \quad \mathrm{IR} \geq -25^\circ\mathrm{C} \end{Bmatrix},$$

$$G = \begin{Bmatrix} \mathrm{LGT} & \text{if} \quad \mathrm{IR} < -25^\circ\mathrm{C} \\ \dfrac{255(0.5\mathrm{VIS} + \mathrm{LGT})}{\max(0.5\mathrm{VIS} + \mathrm{LGT})} & \text{if} \quad \mathrm{IR} \geq -25^\circ\mathrm{C} \end{Bmatrix}, \quad \text{and}$$

$$B = \frac{255\left[\mathrm{LGT} + \dfrac{(255 - \mathrm{IR})}{2}\right]}{\max\left[\mathrm{LGT} + \dfrac{(255 - \mathrm{IR})}{2}\right]}.$$

Use of these data combinations for the different color guns, as seen in Fig. 6, allows lightning to be displayed prominently as white while other visible emission sources appear as orange. Low IR temperatures (high cloud tops) appear as bright blue while high IR temperatures are mapped to low blue values. Most false lightning detections appear in the vicinity of city light edges, fires, or cloud edges in moon-illuminated cases. False detections in high IR temperature regions near these emission sources are minimized by the simple fact that the white (lightning and false detections) and orange (nonlinear emission sources) colors blend relatively well, hiding the false detections. Lightning, on the other hand, occurs most often at low IR brightness temperatures due to lightning's association with phase-stratified clouds (i.e., convection) and, as a consequence, is not obscured by the orange color from other emission sources. To allow for maximum contrast between the detected lightning and the background while maintaining the traditional bright cloud tops and to screen out false detections, visible data are only utilized for regions where the IR brightness temperature is greater than or equal to −25°C. In these regions, only the IR and filtered images are components of the false color image.

b. Comparison to surface observations

We compared the OLS lightning product to data from the NLDN for the case demonstrated in Figs. 3–6. The NLDN utilizes a network of ground-based lightning detectors to find the locations, times, peak current, and multiplicity of cloud-to-ground lightning flashes over, and a few hundred kilometers offshore of, the continental United States (Cummins et al. 1998).

The NLDN and the OLS observe lightning in very different ways. The NLDN is able to constantly monitor its large domain. The OLS is able to detect lightning only when that lightning happens to occur while the sensor is looking at the correct location. Being a polar-orbiting sensor, however, the OLS is capable of covering a much larger (global) spatial domain than is the NLDN. Also, since the OLS views illuminated cloud tops, it is assumed that it is capable of picking up both cloud-to-ground and intracloud lightning (Orville and Henderson

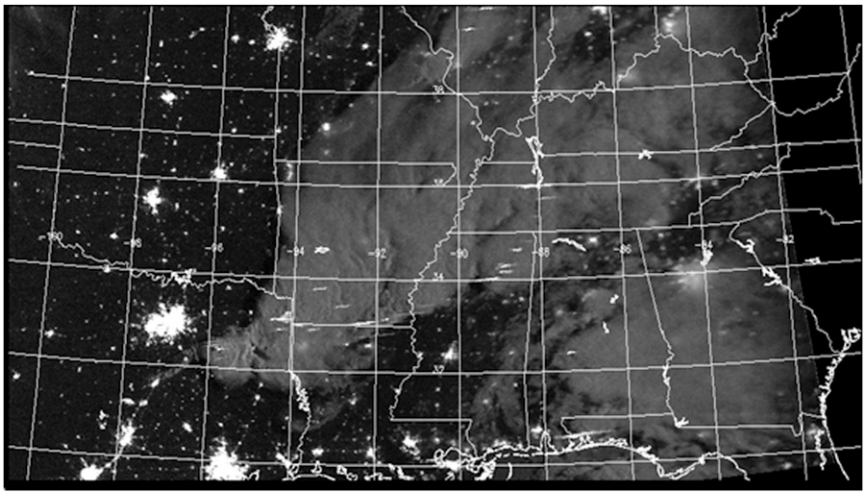

FIG. 7. The OLS nighttime visible image over the southeast United States at 0146 UTC 25 Oct 2010.

1986), but is more sensitive to intracloud flashes. The NLDN, on the other hand, detects primarily cloud-to-ground flashes, likely detecting different lightning flashes from the OLS, even in the same area and during the same time span. In situations in which NLDN and the OLS detect the same lightning flash, the flash will probably be seen in different locations by the two detection methods. The illuminated cloud tops seen by the OLS may extend over many kilometers and the lightning flash itself may not be within the pixels being observed. Also, the lightning flash may extend many kilometers in the horizontal before terminating. As a consequence, there may be a discrepancy between the NLDN detection location and the satellite-observed location. In addition, the ends of scan-line segments saturated by the lightning event can extend well away from the parent cumulonimbus cell in the satellite imagery due to persistence effects. This can result in additional location discrepancies in the two datasets. Finally, parallax effects in the satellite imagery (particularly for thunderstorms near the OLS swath edge) can result in lightning flash location errors of several kilometers unless corrected for geometrically (necessitating an assumption on the location of the flash in the vertical).

These differences in detection methods render difficult the direct comparison between the OLS- and NLDN-detected lightning. Instead, we simply looked for reasonable spatial and temporal correlations between the two detection methods. For this comparison, we selected a spatial domain that best encompassed lightning in the OLS imagery. Considering the potential for location errors for these offshore locations as well as the fact that the flash as noted in the OLS image may be a distance from the strike location (especially for cells covering a large area), the NLDN data were searched for lightning flashes within 50 km and 1 s in time of each OLS pixel, regardless of whether the pixel contained lightning. For the Fig. 3 case, a total of 32 unique lightning flashes were found in the NLDN data positioned close in time and in the vicinity of the corresponding OLS pixels (Fig. 6). While a quantitative comparison is not possible due to the nature of the OLS lightning product and the differences in the detection methodology, it is apparent that the electrically active regions observed by the two detection methods match well with one another.

We also compared our product to the North Alabama Lightning Mapping Array (NALMA), a multisensor network for measuring the VHF radio waves produced by lightning (Koshak et al. 2004). Figures 7–10 show the OLS nighttime visible image, IR image, lightning detection image, and a comparison for the night of 24–25 October 2010. The same considerations that were given to the NLDN comparison in terms of location and timing are applied here as well. Distance and temporal ranges of 50 km and 1 s, respectively, are used. The major difference between the NALMA and the NLDN is that the NALMA is capable of detecting ''total lightning'' (i.e., intracloud and cloud to ground) providing a much more complete view of lightning, but over a much smaller region as shown in red in Fig. 10 (approximately 32.65°N, 89.23°W to 36.79°N, 84.06°W). The detection efficiency decreases further from the center of this network area, as highlighted by the lack of denoted LMA flashes near the western edge of the network boundary.

5. Discussion and conclusions

The unique ability of the OLS sensor to image visible light emissions at night and the characteristics of lightning

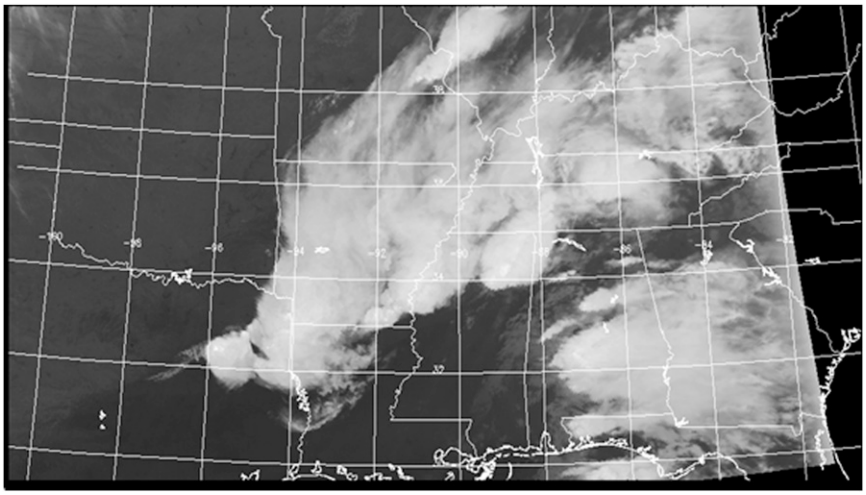

FIG. 8. As in Fig. 7, but for the OLS IR image.

as seen in this imagery has motivated the development of an automated lightning detection algorithm and enhanced lightning detection product. This application of line detection methodology and false color (RGB) compositing can be done under all levels of lunar illumination, resulting in a product that highlights areas of lightning. Without such a technique, faint lightning signatures embedded in strongly illuminated clouds may go undetected by a human analyst.

Comparisons between OLS-detected lightning and data from two ground-based lightning sensor networks (NLDN and NALMA) demonstrate high spatial and temporal correlations, despite comparison challenges. Even if the OLS had the ability to ''stare'' at the entire electrified cloud system via a charge-coupled device (CCD) array, there would still be differences. For instance, the NLDN is sensitive to cloud-to-ground lighting and the OLS detects both cloud-to-ground and intracloud flashes. On the other hand, the NALMA is sensitive to both intracloud and cloud-to-ground lightning, but, while the OLS can detect cloud-to-ground lightning, it is biased toward intracloud lightning. These differences in perspective have been considered in the development of the Geostationary Lightning Mapper (GLM), which is slated to fly on the next-generation Geostationary Operational Environmental Satellite (GOES-R) satellite (Goodman et al. 2010).

Further improvement in the OLS lightning product may be possible through a few different methods. Using other spectral channel data from geostationary satellites,

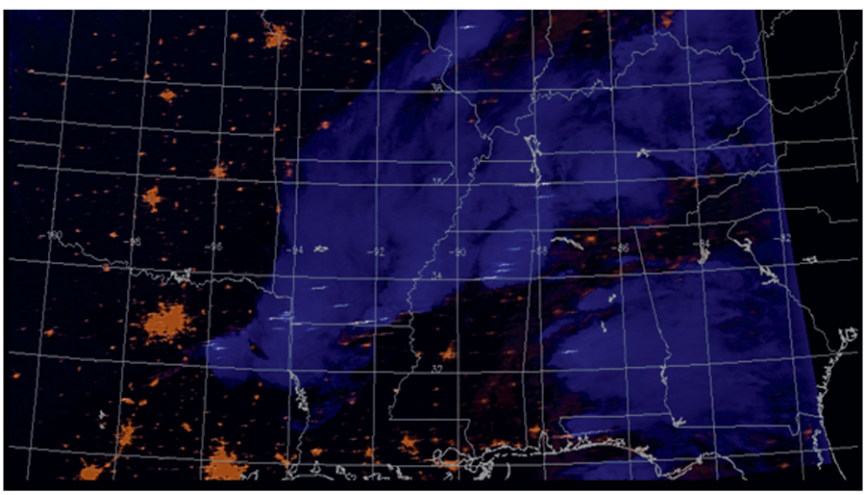

FIG. 9. The RGB composite image of nighttime VIS, IR, and detected LGT imagery data at 0146 UTC 25 Oct 2010.

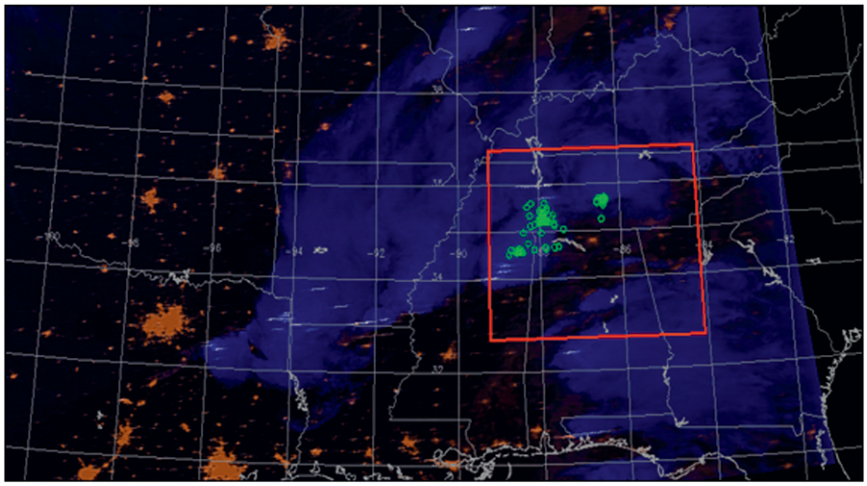

FIG. 10. As in Fig. 9, but with NALMA-detected flashes within the network (red box) indicated with green circles. Only those NALMA-recorded flashes that occurred within 1 s and 50 km of the time and location, respectively, of any OLS pixels within the region are marked.

CO_2 slicing, and other techniques could aid in scene discrimination and allow the algorithm to make decisions based on cloud type (including the presence of thin cirrus), cloud optical depth, and other derived properties. Elimination of false alarms using a precompiled, cloud-free city lights mask is problematic due to the poor navigation of the DMSP satellites, but may still be beneficial. More refined filtering techniques, based on a characteristic brightness curve for lighting or other physical parameters, may also be able to improve the retrievals.

The DMSP OLS is the principal legacy sensor to the future Visible-Infrared Imager-Radiometer Suite (VIIRS) Day/Night Band (DNB) to fly on the NPOESS Preparatory Satellite (NPP) in late 2011. Lee et al. (2006) describe some of the expected VIIRS DNB improvements, including reduced pixel saturation, smaller IFOV (reduced spatial blurring), superior calibration, more accurate geolocation, higher radiometric resolution, a collocation with other VIIRS channels and other sensors on future satellites, and generally increased spatial resolution and decrease in cross-track pixel size variation. These upgrades should lead to corresponding improvements in the techniques available for lightning detection. The increase in spatial resolution could increase the frequency with which lightning is detected due to an increased number of scan lines, but may also create the possibility of viewing the same flash twice. More accurate geolocation will allow for the use of false detection reduction techniques that do not currently work with OLS data (e.g., elimination of false signatures by masking based on known city lights). The availability of additional spectral channels will allow the use of various channel combinations, leading to improvements in lightning flash detection or false alarm removal.

Acknowledgments. The support of the research sponsors, the Office of Naval Research (PE-0602435N) and the Oceanographer of the Navy and PEO C41 and Space/PMW-180 (PE-0603207N), is gratefully acknowledged. Special thanks to NASA SPoRT and Dr. Geoffrey Stano for their contribution in the acquisition and analysis of the NALMA data.

REFERENCES

Bernstein, B. C., F. McDonough, M. K. Politovich, B. G. Brown, T. P. Ratvasky, D. R. Miller, C. A. Wolff, and G. Cunning, 2005: Current icing potential: Algorithm description and comparison with aircraft observations. *J. Appl. Meteor.,* **44,** 969–986.

Boccippio, D. J., K. L. Cummins, H. J. Christian, and S. J. Goodman, 2001: Combined satellite- and surface-based estimation of the intracloud–cloud-to-ground lightning ratio over the continental United States. *Mon. Wea. Rev.,* **129,** 108–122.

Cummins, K. L., M. J. Murphy, E. A. Bardo, W. L. Hiscox, R. B. Pyle, and A. E. Pifer, 1998: A combined TOA/MDF technology upgrade of the U.S. National Lightning Detection Network. *J. Geophys. Res.,* **103,** 9035–9044.

DeMaria, M., and R. T. DeMaria, 2009: Applications of lightning observations to tropical cyclone intensity forecasting. Preprints, *16th Conf. on Satellite Meteorology and Oceanography,* Phoenix, AZ, Amer. Meteor. Soc., 1.3. [Available online at http://ams.confex.com/ams/pdfpapers/145745.pdf.]

Demetriades, N. W. S., R. L. Holle, S. Businger, and R. D. Knabb, 2010: Eyewall lightning outbreaks and tropical cyclone intensity change. Preprints, *29th Conf. on Hurricanes and Tropical Meteorology*, Tucson, AZ, Amer. Meteor. Soc., 16D.3. [Available online at ams.confex.com/ams/pdfpapers/168543.pdf.]

Elvidge, C. D., K. E. Baugh, E. A. Kihn, H. W. Kroehl, and E. R. Davis, 1997: Mapping city lights with nighttime data from the DMSP Operational Linescan System. *Photogramm. Eng. Remote Sens.,* **63,** 727–734.

——, ——, V. R. Hobson, E. A. Kihn, and H. W. Kroehl, 1998a: Detection of fires and power outages using DMSP-OLS data. *Remote Sensing Change Detection: Environmental Monitoring Methods and Applications,* R. S. Lunetta and C. D. Elvidge, Eds., Ann Arbor Press, 123–135.

——, D. W. Pack, E. Prins, E. A. Kihn, J. Kendall, and K. E. Baugh, 1998b: Wildfire detection with meteorological satellite data: Results from New Mexico during June of 1996 using GOES, AVHRR, and DMSP-OLS. *Remote Sensing Change Detection: Environmental Monitoring Methods and Applications,* R. S. Lunetta and C. D. Elvidge, Eds., Ann Arbor Press, 103–121.

Goodman, S. J., R. Blakeslee, W. Koshak, W. A. Petersen, L. Carey, and D. Mach, 2010: The Geostationary Lightning Mapper (GLM) for GOES-R: A new operational capability to improve storm forecasts and warnings. Preprints, *Sixth Symp. on Future National Operational Environmental Satellite Systems—NPOESS and GOES-R,* Atlanta, GA, Amer. Meteor. Soc., 4.2. [Available online at http://ams.confex.com/ams/pdfpapers/158053.pdf.]

Isaacs, R. G., and J. C. Barnes, 1987: Intercomparison of cloud imagery from the DMSP OLS, NOAA AVHRR, and Landsat MSS. *J. Atmos. Oceanic Technol.,* **4,** 647–667.

Koshak, W. J., and Coauthors, 2004: North Alabama Lightning Mapping Array (LMA): VHF source retrieval algorithm and error analyses. *J. Atmos. Oceanic Technol.,* **21,** 543–558.

Lee, T. F., S. D. Miller, F. J. Turk, C. Schueler, R. Julian, S. Devo, P. Dills, and S. Wang, 2006: The NPOESS VIIRS day/night visible sensor. *Bull. Amer. Meteor. Soc.,* **87,** 191–199.

Miller, S. D., and R. E. Turner, 2009: A dynamic lunar spectral irradiance data set for NPOESS/VIIRS day/night band nighttime environmental applications. *IEEE Trans. Geosci. Remote Sens.,* **47,** 2316–2329.

——, A. P. Kuciauskas, M. Liu, Q. Ji, J. S. Reid, D. W. Breed, A. L. Walker, and A. A. Mandoos, 2008: Haboob dust storms of the southern Arabian Peninsula. *J. Geophys. Res.,* **113,** D01202, doi:10.1029/2007JD008550.

Orville, R. E., 1981: Global distribution of midnight lightning—September to November 1977. *Mon. Wea. Rev.,* **109,** 391–395.

——, and R. W. Henderson, 1986: Global distribution of midnight lightning: September 1977 to August 1978. *Mon. Wea. Rev.,* **114,** 2640–2653.

Scharfen, G. R., 1999: Analysis of the U.S. Air Force defense meteorological satellite program imagery for global lightning. NASA Marshall Flight Center Grant NAG8-1093, 7 pp.